Inorganic Chemistry

Communication

pubs.acs.org/IC

^{1}H-ENDOR Evidence for a Hydrogen-Bonding Interaction That Modulates the Reactivity of a Nonheme Fe^{IV}=O Unit

Muralidharan Shanmugam,[†] Genqiang Xue,[‡] Lawrence Que, Jr.,*[,‡] and Brian M. Hoffman*[,†]

[†]Department of Chemistry, Northwestern University, Evanston, Illinois 60208-3113, United States

[‡]Department of Chemistry and Center for Metals in Biocatalysis, University of Minnesota, Minneapolis, Minnesota 55455, United States

Supporting Information

ABSTRACT: We report that a novel use of 35 GHz ^{1}H-ENDOR spectroscopy establishes the presence in **1** of an Fe^{IV}=O···H−O−Fe^{III} hydrogen bond predicted by density functional theory computations to generate a six-membered-ring core for **1**. The hydrogen bond rationalizes the difference in the C−H bond cleavage reactivity between **1** and **4**(OCH_3) (where a CH_3O group has replaced the HO on the Fe^{III} site). This result substantiates the seemingly paradoxical conclusion that the nonheme Fe^{IV}=O unit of **1** not only has the electrophilic character required for H-atom abstraction but also retains sufficient nucleophilic character to accept a hydrogen bond from the Fe^{III}−OH unit.

Hydrogen bonding is an essential element in Nature's toolbox for stabilizing structures and modulating the reactivity. The key roles played by hydrogen bonding in the catalytic sites of iron proteins are particularly well illustrated by their contrasting effects on their interaction with O_2. Hydrogen bonds to O_2 as an iron ligand serve to maintain reversible O_2 binding in hemoglobin and hemerythrin, whereas hydrogen bonds promote O−O bond cleavage in monooxygenases such as cytochrome P450.[1−4] Hydrogen bonding to nonheme metal−oxo units may also be important. Indeed, Borovik et al. have elegantly demonstrated the significance of intramolecular hydrogen bonds in stabilizing the first crystallographically characterized, synthetic oxoiron(III) complex.[5] Oxidizing the oxoiron(III) center to its iron(IV) counterpart significantly weakens hydrogen bonds to the Fe^{IV}=O center,[6] but how this affects the reactivity of the Fe^{IV}=O unit has not been determined.

In our efforts to obtain a synthetic model for high-valent intermediate **X** in the activation cycle of class 1a ribonucleotide reductases, we generated complex **1** (Scheme 1), which has the Fe^{III}−O−Fe^{IV} core found in **X** and exhibits electron paramagnetic resonance (EPR) and Mössbauer spectra very similar to those of **X**.[7−11] Complex **1** can be obtained by the nucleophilic attack of hydroxide ion on the [$Fe^{III}Fe^{IV}(\mu$-O)$_2$] diamond core of **2**, generating the open HO−Fe^{III}−O−Fe^{IV}=O core of **1**. The closely related **4**(OCH_3) can be generated by a similar reaction with methoxide and exhibits similar spectroscopic features.[12] Interestingly, H-atom transfer to **4**(OCH_3) from 9,10-dihydroanthracene occurs 13-fold faster at −80 °C than that to **1**. It was postulated that this difference

Scheme 1

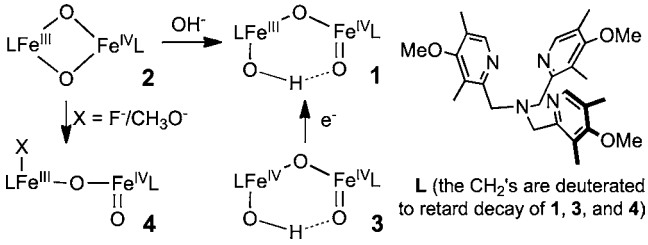

occurs because a hydrogen bond in **1** between the H atom of Fe^{III}−OH and the O atom of the terminal Fe^{IV}=O (Scheme 1) diminishes the electrophilicity of Fe^{IV}=O.[12] Although density functional theory (DFT) computations provide support for such an interaction,[11] there is no direct experimental evidence for this pivotal hydrogen bond in the condensed phase. Given the high reactivity of **1**, it is unlikely that it can be crystallized. Therefore, we have employed ^{1}H-ENDOR spectroscopic studies of **1** to establish the spatial relationship of the O−H proton to the two Fe atoms of **1**, thereby proving the existence of the six-membered ring whose formation is driven by this hydrogen bond. This hydrogen bond is further discussed as a central element in the interpretation of the C−H bond cleavage reactivity of this unique high-valent complex.

Complex **1**(OH/OD), like intermediate **X**, exhibits an $S = {}^1/_2$ ground state as a result of antiferromagnetic spin coupling between the high-spin Fe^{III}($S = {}^5/_2$)/Fe^{IV}($S = 2$) ions. Its 35 GHz EPR spectrum is described by the **g** tensor [2.008, 2.003, 1.992], comparable to that of **X**.[11,13] The spectrum shows a small variability in $g_{1/2}$ that is assigned to solvent/freezing effects (Figure S1 in the Supporting Information, SI).[10,14−16]

Davies Q-band ^{1}H-ENDOR spectra[15,16] of **1**(OH/OD) collected at $g = 2.003$ show signals centered at the ^{1}H Larmor frequency from ^{1}H with a range of couplings (Figure 1). The most strongly coupled signal, $A_{max}(^1H_A) \sim 35$ MHz, is partially lost in the **1**(OD) sample[14,17] (Figures 1 and S2 in the SI), identifying it with the Fe^{III}−OH proton, ^1H_A. Protons associated with the supporting organic ligand, hyperfine couplings $A \leq 10$ MHz, do not exchange.[17]

Figure 2 shows the 2D field-frequency plot of Davies ^{1}H-ENDOR spectra of **1**(OH), collected at numerous fields across the EPR envelope. At $g_1 = 2.01$ the ^1H_A doublet exhibits a

Received: July 19, 2012
Published: September 17, 2012

   dx.doi.org/10.1021/ic3015783 | *Inorg. Chem.* 2012, 51, 10080−10082

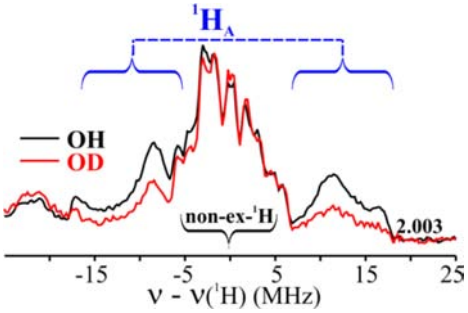

Figure 1. Davies ^{1}H-ENDOR spectra of **1**(OH/OD) at g = 2.003. The blue curly brackets show the ^1H_A signal. Conditions: π-pulse length = 120 ns, τ = 600 ns, repetition time = 40 ms, microwave frequency = 34.698 GHz, and T = 2 K.

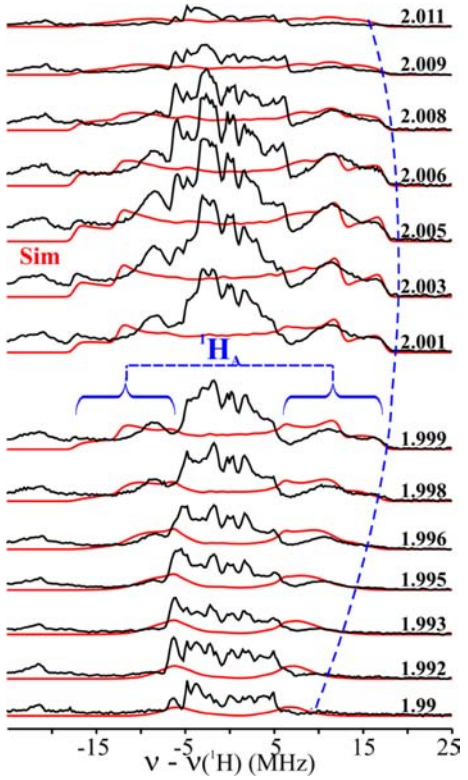

Figure 2. Simulated (red lines; see the text for simulation parameters and Table S1 in the SI) and experimental (black lines) 2D field-frequency plot of Davies ^{1}H-ENDOR spectra of **1**(OH). Conditions: as in Figure 1.

hyperfine coupling of $\mathbf{A}(^1H_A) \sim 25$ MHz. As the field is increased, the $\nu^+ = [\nu(^1H) + \mathbf{A}(^1H_A)/2]$ branch of the ^1H_A signal intensifies as a shoulder develops to high frequency and becomes a peak with maximum hyperfine coupling of $\mathbf{A}(^1H_A) \sim 35$ MHz at $g \sim 2.005$.[18] Upon further increase in the field, the shoulder collapses, and the ν^+ feature again becomes a single peak at g_3 = 1.992.

Previous studies have shown that the anisotropic hyperfine interaction component for a proton in a dinuclear center such as **1**(OH) is determined by electron−nuclear point−dipole interactions between the proton and the spin-coupled Fe ions and that this component can be calculated from the metrical parameters of the Fe^{III}−H−Fe^{IV} fragment.[13,19,20] Simulation of the 2D ENDOR pattern of ^1H_A signals collected at fields across the EPR envelope of **1** thus began by calculating the dipolar interaction tensor, $\mathbf{T}_{cal}$, from metrical parameters derived from the DFT-optimized structure of **1**: Fe^{III}−Fe^{IV} distance d_{Fe-Fe} = 3.34 Å; parameters defining the −OH proton position relative to the two Fe ions, r_1 = 2.38 Å, β_1 = 56.6° (Figure 3 and Table

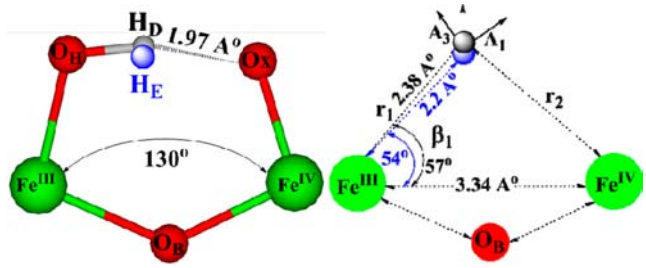

Figure 3. (left) Structural description of ENDOR ($\mathbf{H}_E$) and DFT-optimized ($\mathbf{H}_D$) locations of ^1H_A of **1**. (right) Definitions of metrical parameters used to calculate the cluster dipolar interaction tensor **T**.

S1 in the SI). With the resulting tensor $\mathbf{T}_{cal}$ = [−9.0, −22.4, +31.4] MHz taken as the starting point, the isotropic coupling a_{iso}, anisotropic tensor components $\mathbf{T}_{ex,i}$, where i = 1−3, and orientation of the experimental hyperfine tensor $\mathbf{T}_{ex}$, relative to the **g** tensor, were varied until simulations matched the experimental 2D pattern of ^1H_A ENDOR signals. Overlaid on the experimental spectra (Figure 2) are the excellent simulations computed with the optimized hyperfine tensor $\mathbf{A}(^1H_A) = a_{iso}(^1H_A) + \mathbf{T}_{ex}(^1H_A) = -0.73 + [-11.3, -24.3, +35.6]$ MHz (orientation relative to **g**, α = 30.0°, β = 60.0°), which is dominated by the anisotropic term $\mathbf{T}_{ex}(^1H_A)$.

Through use of the point−dipole equations,[19−22] the experimentally derived $\mathbf{T}_{ex}(^1H_A)$ can, in turn, be used to infer the actual geometry of the Fe^{III}−H−Fe^{IV} fragment. $\mathbf{T}_{ex}(^1H_A)$ differs slightly from $\mathbf{T}_{cal}$ derived from the DFT structure, but the experimental tensor is precisely matched by a proton position that is minimally different from that of the DFT-optimized structure: r_1 = 2.20 Å; β_1 = 54° (Figure 3 and Table S1 in the SI). Most importantly, simulations with a linear Fe^{III}−O−Fe^{IV}, with ^1H_A rotated about the Fe^{III}−O_H bond, or even with a bridging hydroxo, completely fail to reproduce the ENDOR results (Figures S5−S8 and Tables S1 and S2 in the SI).

The ENDOR results thus provide strong experimental evidence in support of the DFT-optimized structure of **1**, which shows the oxo ligand of the Fe^{IV} ion and ^1H_A of the hydroxo ligand on the Fe^{III} ion at a distance indicative of Fe^{IV}═O···H−O−Fe^{III} hydrogen bonding. This interaction decreases the Fe^{III}−O−Fe^{IV} angle to 130.0°, from the value 175.0° calculated for **4**(F) (and by extension to **4**−OCH_3), complexes for which such hydrogen bonding and formation of a closed cycle are precluded.[11] Likewise, the hydrogen-bonding interaction reduces the dihedral angle in the DFT-optimized structure O_x═Fe^{IV}−Fe^{III}−O_H to 32.0°, whereas it is 180.0° for **4**(F).[11] The position of the hydroxyl proton, ^1H_A(**E**), determined by ENDOR measurements of **1** in a frozen solution is the same as that of the proton in the DFT-generated structure, ^1H_A(**D**), within the accuracy of measurements/analysis, and thus the ENDOR measurement confirms the presence in a frozen solution of the Fe^{IV}═O···H−O−Fe^{III} hydrogen bond predicted by DFT to drive Fe−O−Fe bending in **1** required to generate the cyclic structure.

Additional corroboration of this conclusion derives from the observation that chemical reduction or cryoreduction of **3** also

dx.doi.org/10.1021/ic3015783 | Inorg. Chem. 2012, 51, 10080−10082

afforded **1**. Precursor **3** has been characterized to be a (μ-oxo)diiron(IV) complex with an EXAFS-determined Fe−Fe distance of 3.32 Å, implicating a bent Fe−O−Fe unit with an Fe−O−Fe angle of ca. 130°.[23] One-electron reduction of **3** thus occurs without an appreciable change in the net Fe−Fe distance.[10,11]

This Communication reports a novel use of 35 GHz ^{1}H-ENDOR spectroscopy to precisely probe the solution-phase structure of **1**. Metrical parameters derived from ENDOR measurements verify the bending of the Fe−O−Fe linkage predicted by DFT computations and thus establish the presence of the predicted $Fe^{IV}{=}O_x{\cdots}H{-}O{-}Fe^{III}$ hydrogen bond that drives this bending and generates the cyclic, six-membered-ring core of **1**. Indeed, the ENDOR results provide the only direct experimental evidence that proves the existence of this hydrogen bond. Its existence in **1** rationalizes the difference in the C−H bond cleavage reactivity between **1** and **4**(OCH_3).[12] Loss of this hydrogen bond upon replacement of the terminal hydroxide on the Fe^{III} center of **1** with a methoxide ligand in **4**(OCH_3) unmasks the full H-atom-abstraction potential of the Fe^{IV}=O unit. By establishment of the postulated hydrogen bond to the oxo group of **1**, this study thus substantiates the seemingly paradoxical conclusion that the nonheme Fe^{IV}=O unit not only has the electrophilic character required for H-atom abstraction but also retains the nucleophilic character needed for a hydrogen-bond acceptor. Such hydrogen-bonding interactions thus are shown to be useful in modulating the reactivity of high-valent iron oxo species generated in an enzyme active site.

■ ASSOCIATED CONTENT

Ⓢ Supporting Information

Eight figures (EPR and ENDOR) and two tables. This material is available free of charge via the Internet at http://pubs.acs.org.

■ AUTHOR INFORMATION

Corresponding Author

*E-mail: bmh@northwestern.edu (B.M.H.), larryque@umn.edu (L.Q.).

Notes

The authors declare no competing financial interest.

■ ACKNOWLEDGMENTS

This work was supported by the National Institutes of Health (Grant GM38767 to L.Q. and Grant HL 13531 to B.M.H.).

■ REFERENCES

(1) Denisov, I. G.; Makris, T. M.; Sligar, S. G.; Schlichting, I. *Chem. Rev. (Washington, DC)* **2005**, *105*, 2253−2277.

(2) Davydov, R.; Hoffman, B. M. *Arch. Biochem. Biophys.* **2011**, *507*, 36−43.

(3) Shiemke, A. K.; Loehr, T. M.; Sanders-Loehr, J. *J. Am. Chem. Soc.* **1986**, *108*, 2437−2443.

(4) Kurtz, D. M. *Chem. Rev.* **1990**, *90*, 585−606.

(5) MacBeth, C. E.; Golombek, A. P.; Young, V. G., Jr.; Yang, C.; Kuczera, K.; Hendrich, M. P.; Borovik, A. S. *Science (Washington, DC)* **2000**, *289*, 938−941.

(6) Lacy, D. C.; Gupta, R.; Stone, K. L.; Greaves, J.; Ziller, J. W.; Hendrich, M. P.; Borovik, A. S. *J. Am. Chem. Soc.* **2010**, *132*, 12188−12190.

(7) Fe ions of **2**−**4** are low-spin, but in **1**, they are high-spin and spin-coupled to give a $S = {}^1/_2$ ground state.

(8) Sturgeon, B. E.; Burdi, D.; Chen, S.; Huynh, B. H.; Edmondson, D. E.; Stubbe, J.; Hoffman, B. M. *J. Am. Chem. Soc.* **1996**, *118*, 7551−7557.

(9) Burdi, D.; Willems, J.; Riggs-Gelasco, P.; Antholine, W.; Stubbe, J.; Hoffman, B. *J. Am. Chem. Soc.* **1998**, *120*, 12910−12919.

(10) Xue, G.; De Hont, R.; Muenck, E.; Que, L., Jr. *Nat. Chem.* **2010**, *2*, 400−405.

(11) De Hont, R. F.; Xue, G.; Hendrich, M. P.; Que, L.; Bominaar, E. L.; Munck, E. *Inorg. Chem. (Washington, DC)* **2010**, *49*, 8310−8322.

(12) Xue, G.; Pokutsa, A.; Que, L. *J. Am. Chem. Soc.* **2011**, *133*, 16657−16667.

(13) Shanmugam, M.; Doan, P. E.; Lees, N. S.; Stubbe, J.; Hoffman, B. M. *J. Am. Chem. Soc.* **2009**, *131*, 3370−3376.

(14) **1**(OH/OD) was prepared by the reduction of **3** with 1 equiv of ferrocene in 3:1 CH_2Cl_2/CH_3CN at −85 °C.[10] **3** was prepared by the reaction of its diferric precursor with 1 equiv of H_2O_2, with the maximum yield obtained with exactly 1 equiv of H_2O_2. The solutions of **1**(OH/OD) were quickly transferred into ENDOR tubes in dry ice and frozen in liquid N_2. The presence of some **1**(OH) in the **1**(OD) sample is ascribed to H/D exchange with residual H_2O from a diferric precursor and solvent present at concentrations comparable to that of the 1 equiv of D_2O_2 (~10% in D_2O, 98% d) added to generate **3**(OD). Diferric impurities from the decay of **1**, unreacted precursor, and a ferrocenium byproduct are EPR/ENDOR-silent. Davies Q-band pulsed EPR/ENDOR measurements were performed as described.[15,16]

(15) Zipse, H.; Artin, E.; Wnuk, S.; Lohman, G. J. S.; Martino, D.; Griffin, R. G.; Kacprzak, S.; Kaupp, M.; Hoffman, B.; Bennati, M.; Stubbe, J.; Lees, N. *J. Am. Chem. Soc.* **2009**, *131*, 200−211.

(16) Davoust, C. E.; Doan, P. E.; Hoffman, B. M. *J. Magn. Reson.* **1996**, *119*, 38−44.

(17) ^2H_A ENDOR was not detected for **1**(OD) because the signals overlap with strong ^{14}N signals from the eight coordinating ligand N atoms (Figures S3 and S4 in the SI).

(18) The $\nu^- = [\nu(^1H) - \mathbf{A}(^1H_A)/2]$ branch of ^1H_A doublet is of lower intensity because of relaxation effects.

(19) DeRose, V. J.; Liu, K. E.; Lippard, S. J.; Hoffman, B. M. *J. Am. Chem. Soc.* **1996**, *118*, 121−134.

(20) Willems, J.-P.; Lee, H.-I.; Burdi, D.; Doan, P. E.; Stubbe, J.; Hoffman, B. M. *J. Am. Chem. Soc.* **1997**, *119*, 9816−9824.

(21) The spin density on individual Fe ions was taken as $\rho \sim 0.9$ to account for delocalization to ligands.[22]

(22) Tierney, D. L.; Martásek, P.; Doan, P. E.; Masters, B. S.; Hoffman, B. M. *J. Am. Chem. Soc.* **1998**, *120*, 2983−2984.

(23) Xue, G.; Fiedler, A. T.; Martinho, M.; Munck, E.; Que, L., Jr. *Proc. Natl. Acad. Sci. U.S.A.* **2008**, *105*, 20615−20620.